

Application of ion exchange resins to reduce hardness and scaling of drinking water: Experimental and modeling

Shahla Sadeghi¹, Mohsen Abbasi^{*1}, Shahriar Osfouri¹, Mohammad Javad Dianat¹ and Javad Khodaveisi²

¹Department of Chemical Engineering, Faculty of Petroleum, Gas and Petrochemical Engineering, Persian Gulf University, 75169, Bushehr, Iran

²Water and Wastewater Company of Bushehr Province, Bushehr, Iran

(Received March 16, 2020, Revised May 6, 2021, Accepted September 15, 2021)

Abstract. In this research, the performance of strong cationic Purolite C-100 Na⁺, Ambersep IR252 H⁺, Amberlite IR120 H⁺ ion exchange resins and an IRA402 OH⁻ anionic resin have investigated to the reduction of hardness and TDS of drinking water in Bushehr, Iran. Also, to demonstrate the efficiency of these resins, the experimental variables affecting the ion exchange process such as contact time and adsorbent consumption were investigated. The results showed that the maximum adsorption capacity in the best operating condition was 48.01, 45 and 36.01 mg.g⁻¹ for Purolite, Ambersep, and Amberlite resins, respectively. The maximum percentage of total hardness reduction parameters, calcium and magnesium ions reduction at best operating condition was 90.086%, 93.085%, 77.27% for Purolite ion exchange resins, 83.84%, 86.70%, 71.59% for Ambersep ion exchange resins and 69.83, 69.41, 69.32 for Amberlite ion exchange resins, respectively. Also, in the compound stage (the combination of cationic and anionic resins), at the best condition, 3 g/L of cationic resin and 12 g/L of anionic resin had the best efficiency in adjusting pH and reducing TDS. To study the adsorption kinetic process of calcium and magnesium ions by three strong cationic ion exchange resins, three pseudo-first-order, pseudo-second-order, and Morris-Weber models were employed. Among these models, the pseudo-second-order kinetic model had the best agreement with the experimental data. The models of Langmuir, Freundlich, Temkin, and Dobinin-Radskvich were utilized for the equilibrium study of hardened ions adsorption (calcium and magnesium). From the equilibrium study of the absorption process, it was founded that this process involves both chemical and physical absorption and the Langmuir model has the best agreement with the experimental data.

Keywords: hardness; ion exchange resins; scaling; TDS; water corrosion

1. Introduction

Because the total dissolved solids (TDS) and hardness in water reduce the quality of drinking water and cause problems such as corrosion and scaling in the pipelines, which costs a lot, various investigations are needed to reduce TDS and hardness in drinking waters. In this regard, finding effective and economical adsorbents is essential for reducing water hardness and TDS in terms of industrial or drinking water (Asl *et al.* 2013, Gupta and Bhattacharyya 2008, Katal and Pahlavanzadeh 2011, Lv *et al.* 2019). The phenomenon of ion exchange as an efficient and economical method for the reduction of TDS and hardness in water was introduced for the first time by Thomson and Wye on the exchangers (Cornelissen *et al.* 2009, Helms 1973, Khan *et al.* 2016, 2018, Prajapati *et al.* 1983, Townsend 1993). Duncan and Lister (1948) introduced two new ionic exchangers to the industry, cationic exchange as a phenol-aldehyde and anionic exchange as a product of polyamines and aldehyde form (Özmetin and Aydin 2007, Özmetin *et al.* 2009). Subsequently, many researchers investigated the of ion exchange: (Ambashta and Sillanpää

2010, Apell and Boyer 2010, Benefield *et al.* 1982, Coca *et al.* 2010, Entezari and Tahmasbi 2009, Sepehr *et al.* 2013, Yu *et al.* 2015, Zainol and Nicol 2009). Entezari *et al.* (2009) researched to reduce the hardness of water using the combination of ion exchange and sonication methods. They investigated variables such as the intensity of ultrasound, amount of resin, the concentration of ions, and contact time. They found that kinetic removal for magnesium and calcium ions was pseudo-first-order, and experimental data was fitted with the Langmuir model. Zainol *et al.* (2009) examined the cation exchange equilibrium of nickel, cobalt, manganese, and magnesium with acidic resin IMR 784 amberlite. They observed that the amount of metal absorbed by the resin enhances with increasing pH. Özmetin *et al.* (2009) presented an experimental kinetic model for the removal of pure calcium, including a saturated boric acid solution, by ion exchange method using a strong acidic cation exchange resin (IR120 amberlite). The results of their research show that it is necessary to study the effects of process variables with environmental benefits such as price and industrial application.

Cornelissen *et al.* (2009) used IIX ion exchange resins as pre-treatment to control clogging in ultrafiltration membranes. Anionic resins are effective in treating surface water with a large amount of suspended matter. Apell and Boyer (2010) carried out studies using a hybrid ion exchange technique to remove soluble organic matter and

*Corresponding author, Ph.D.,
E-mail: m.abbasi@pgu.ac.ir

hardness. They were able to reduce 70 % soluble organic matter and more than 55% hardness by using a cationic and anionic exchange resin. Agakhani *et al.* (2011) used anionic amberlit cationic resin (IR-10 and IRA-402) to absorb calcium and magnesium in saline water. The removal of calcium and magnesium ions in cationic resin was 80.8% and 94.1% respectively, and the result for anionic resin was 76.9% and 47.1% respectively. Zuo *et al.* (2013) carried out studies on the multiplier ion competition migration behavior and their effects on ion exchange resins. The removal rate was reported to be about 99% for 50 hours (EC<0.5 ms/cm). Also, Comstock *et al.* (2014) conducted a research using a combination of magnetic ion exchange and cation exchange to remove hardness and dissolved organic carbon (DOC). They used a magnetic anion exchange resin MIEX-CL and cation exchange resin C-Na-A200. In groundwater treatment, the combined ion exchange method achieved 76% DOC and 97% de-desulfurization using a 20% sodium chloride solution. Also, Millar *et al.* (2014) identified the basic equilibrium behavior of calcium exchange with sodium exchanged weak acid cationic resins. Their results showed that the ion exchange process could exhibit relatively complex behavior and loading of calcium ions was determined equal to 53.5-58.7 g/kg. As another work, Millar *et al.* (2015) studied the ion exchange treatment of saline solutions using a strong acid cationic resin. The matching of equilibrium data with the efficiency of the absorption models showed that the best adaptation is gained using the Freundlich model (Millar *et al.* 2015). Hayani *et al.* (2016) investigated softening of hard water in Morocco by exchanging ions with a Duolit206A strong acid cationic resin. The results showed 63-70% and 54-55% reduction of calcium and magnesium ions in 20 min using 20 g of resin. Furthermore, Ismail (2016) investigated the calcium exchange rate in the process of water softening using a strong acid resin (DOWEX HCR S/S). He concluded that increasing superficial velocity has a negative effect on the ion exchange efficiency.

The purpose of this research is to evaluate the efficiency of different ion exchange resins (sodium and hydrogen form) to reduce TDS and water hardness of drinking water in Bushehr city, Iran. The results of this research can lead to commercializing and reducing the cost of water purification for safe and suitable drinking water to prevent corrosion and scaling and reducing waste of time and cost.

2. Material and methods

The physical and chemical characteristics of the commercial resins that were employed in the experiments are reported in Table 1. To determine the hardness of water during experiments, titration was performed using a buffer solution of ammonium, a normal sodium hydroxide, a trichrome black tetraformate, and an Ethylenediamine tetraacetic acid (EDTA) standard solution. For determining the alkalinity of the samples, the titration method was performed using methyl orange and TIME and a standard solution of 0.02 N sulfuric acid.

Fig. 1 presents the schematic of the experimental setup

used in the experiments. In this research, the tests were conducted in two stages. In the first stage, the performance of three strong cationic ion exchange resins (Purolite C-100 Na⁺, Amberlite IR120 H⁺ and Ambersep IR252 H⁺) was investigated, separately. For each resin, reduction of magnesium and calcium hardness was determined by titration and TDS reduction was calculated by weight estimation. All of the absorption tests were performed in batch model. Initially, the ion exchange resins used in these experiments with different concentrations (1, 2, 3, and 4 gram) were added to the 1-liter beaker containing water samples. The beaker was placed on the stirrer at a constant rotation speed of 350 rpm. After elapsing the contact time (10, 20, 30, 40, 50, 60, and 70 min) and carrying out the adsorption process, the sample was removed from the stirrer and it takes 5 to 7 min for the total precipitation of resin. Then, the solution and ion exchange resin were separated and filtered from the filter paper and prepared for analysis. Afterward, the experimental data were analyzed with four adsorption isotherm models as well as three kinetic models of the reaction. Each test repeated three times to show the reliability of data, and ultimately, the standard deviation for each test was calculated. In the second stage, the combination performance of cationic H⁺ and anionic OH⁻resins were investigated. Experiments were carried out at a concentration of 3 g/L of cationic resin (which was optimized from the first stage) and different concentrations of anionic resin (3, 6, 9, and 12 g/L) at different contact times (10, 20, 30, 40, 50, 60, and 70 min).

For measuring the total hardness of water, 25 ml of water was poured into a beaker and 1 cc of ammonium buffer was added to the desired water to keep the pH constant and a few drops of Eriochrome Black T (EBT) reagent was added. EBT produced a red complex with calcium and magnesium cations at a pH of 10. This complex was broken by the addition of EDTA, which caused the release of EBT and the color of the sample was blue. This state indicated that the titration operation was finished. The total hardness was calculated in terms of calcium carbonate using the Eq. (1):

$$\text{Total Hardness} = \frac{V \times f_c \times 1000}{V_c} \quad (1)$$

where, V is consumption volume (mL), f_c is normality of EDTA and V_c is sample volume (mL).

For measuring the calcium hardness of water, 25 mL of the sample was added into a 250 mL beaker, then 1 to 2 drops of sodium hydroxide solution (1 N) and a sufficient amount of moraxid reagent were added, finally the sample color changed to pink color. The titration was continued using a standard EDTA solution (1 M) until a purple color was formed. The consumed titrant volume was recorded and the calcium hardness was calculated using the Eq. (2):

$$Ca^{2+} = \text{Calcium Hardness as } \frac{mg}{L} CaCO_3 \times 0.4004 \quad (2)$$

Magnesium hardness was obtained by reducing the total hardness and the hardness of calcium according to the Eq. (3). Also, the Eq. (4) was used to obtain the concentration

Table 1 The properties of commercial resins that were used in the experiments

Resin	Amberlite IR120H ⁺	IRA 402 OH ⁻	Ambersep IR252 H ⁺	Purolite C-100
Resin type	Strong cationic	Strong anionic	Strong cationic	Strong cationic
Ionic Form	H ⁺ form	OH ⁻ form	H ⁺ form	Na ⁺ form
PolymerStructure	Styrene divinyl benzene copolymer	Polystyrene divinylbenzene copolymer	Styrene divinylbenzene copolymer	Styrene divinylbenzene copolymer
Functional Group	Sulfonic Acid	Quaternary ammonium	SO ₃ ⁻	Sulfonic Acid
Particle size (mm)	0.62-0.83	0.65-0.85	0.9-1.1	0.3-1.2
Total exchanging capacity (eq/l)	1.80	0.95	1.65	2
Moisture	53-58%	-	52-58%	44-48%
Uniformity Coefficient (Max)	1.8	1.6	1.4	1.7

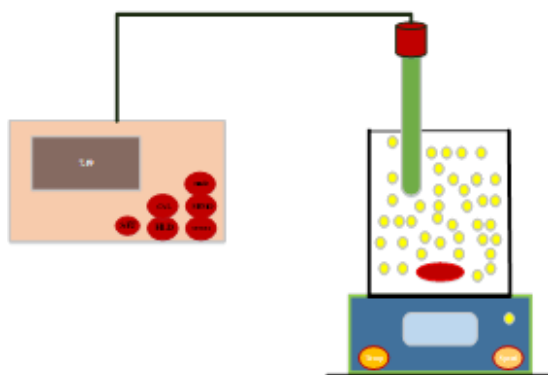


Fig.1 The schematic of the experimental setup

of magnesium ion. APHA (1912).

$$\text{Magnesium Hardness} = \text{Total Hardness} - \text{Calcium Hardness} \quad (3)$$

$$Mg^{2+} = (\text{TotalHardness} - \text{CalciumHardness}) \times 0.24 \quad (4)$$

3. Results and discussion

In this section, the potential of corrosion and sedimentation of drinking water in Bushehr city, Iran, were investigated using the Langelier, Ryznar, Aggressive, and Puckorius indexes. Then, the effects of contact time and different concentrations of adsorbent were investigated on the batch experiments by various ion exchange resins. Finally, the results of experiments analyzed to measure the reduction of the total hardness, especially hardened ions (calcium and magnesium). Also, the kinetic and equilibrium study of the adsorption process using different kinetic and isotherm models were investigated.

3.1 Investigating the potential of drinking water in Bushehr city using corrosion and sedimentation indexes

The tendency of water to corrosion and sedimentation was determined by examining water stability. Stable water

tends to corrode and precipitate slightly, and its values vary for the type of use. The application of corrosion indices is an indirect method in measuring and simply detecting the tendency of water to corrosion and sedimentation. Common indices are: Langlier Saturation Index (LSI), Ryznar Stability Index (RSI), Aggressive Index (AI) and Puckorius Index (PI). Perform control measures (Shams *et al.* 2012), (Vairavamoorthy *et al.* 2007). Using the Eq. 5 to 11 the values of the indicators were calculated (Ebrahimi *et al.* 2012, Hadi 2010).

$$LSI = pH - pH_s \quad (5)$$

$$RSL = 2(pH_s) - pH \quad (6)$$

where, pH is the actual pH of water, pH_s is saturated pH with calcium carbonate. The pH_s was calculated according to the relation 7 to 11.

$$pH_s = (9.3 + A + B) - (C + D) \quad (7)$$

$$A = \frac{\log_{10}([TDS] - 1)}{10} \quad (8)$$

$$B = -13.2 \times \log_{10}(T(^{\circ}C) + 273) + 34.55 \quad (9)$$

$$C = \log_{10}(TH) - 0.4 \quad (10)$$

$$D = \log_{10}(TA) \quad (11)$$

where, TDS is total dissolved solids (mg/L), TH is total hardness (mg/L), TA is total alkalinity (mg/L)

$$AI = [pH + \log[(TA) \times (CH)]] \quad (12)$$

where, CH is Calcium Hardness (mg/L)

$$PI = 2pH_s - pH_{eq} \quad (13)$$

where, pH_{eq} is Water pH in equilibrium

$$pH_{eq} = 1.465 \log(TA) + 4.54 \quad (14)$$

Table 2 The results of chemical quality analysis of drinking water of the Bushehr city

Parameters	Unit	Minimum	Maximum	Average
Temperature	°C	25	27	26
pH	-	7.65	7.85	7.75
Total Alkalinity	mg/L CaCO ₃	66	95	80.5
TDS	mg/L	615	997.12	806.06
Ca ²⁺	mg/L	150.4	195	172.7
Mg ²⁺	mg/L	19.2	21.12	20.16
Total hardness	mg/L CaCO ₃	464	515	489.5

Table 3 Interpretation of corrosive and water sedimentation indexes

Index	Index Value		
Langlier saturation index	$LSL > 0$	$LSL = 0$	$LSL < 0$
	Sedimentation	Stable	Corrosive
Ryznar stability index	$RSL > 6$	$6 < RSL < 7$	$RSL < 6$
	Sedimentation	Stable	Corrosive
Aggressive index	$AL > 12$	$10 < AL < 12$	$AL < 0$
	Highly corrosive	Moderate corrosive	No corrosive
Puckorius index	$PI < 6$	$PI > 6$	Sedimentation
	Corrosive		

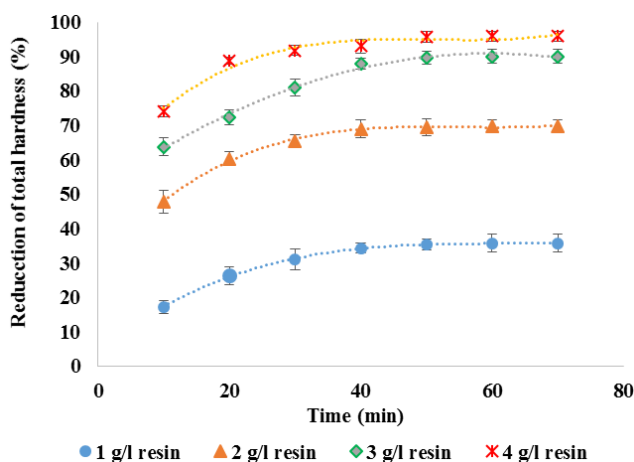
Fig. 2 The reduction of total hardness versus contact time using Purolite C-100 Na⁺ at 25°C and 350 rpm

Table 2 presents the values of the quality parameters of the water sample including pH and total soluble solids (TSS), temperature, calcium ion, and alkalinity. According to the results, the values of Langlier, Ryznar, Aggressive, and Puckorius indexes that identified in Table 3, determined to 0.03, 7.66, 12.22 and 8.02, respectively. Therefore, based on these indexes, it can be concluded that water is corrosive and has a tendency for sedimentation in pipelines and vessels.

3.2 Reducing water hardness using strong cationic ion exchange resins

Fig. 2 illustrates the removal percentage of total hardness, calcium, and magnesium ions at different contact times (10, 20, 30, 40, 50, 60 and 70 min) with various concentrations of Purolite C-100 Na⁺ resin (1, 2, 3, and 4 g/L).

Fig. 2 shows the effect of contact time on the removal percentage of total hardness by various concentrations of Purolite C-100 Na⁺ resin. As seen in Fig. 2, the reduction percentage of total hardness enhanced with increasing contact time. This trend continues until the process reaches equilibrium and then showed a stable trend with little change. In justifying this phenomenon, it can be said that at the beginning of the ionic exchange process, with increasing contact time, the absorbed ions have more chance of penetrating the adsorbent and occupy active adsorbent sites, but when the process reaches to the equilibrium condition, the adsorbent is saturated and filled with adsorbent vacant sites, and increasing the duration of the contact time had no effect on the absorption efficiency. Therefore, increasing the contact time of more than 60 min did not affect the effectiveness of the removal and the best contact time of experiments can be 60 min. According to these figs, the removal percentage of total hardness with a concentration of 1 g/L of resin was equivalent to 35.78%, 2 g/L of resin to 69.83%, 3 g/L to 90.86% and 4 g/L to 95.95%. Therefore, according to the results and by considering cost of resins, 3 g/L concentration can be regarded as a suitable concentration during the ionic exchange process. Therefore, this resin was suitable for the removal of water hardness, since it has a high removal percentage and also maintains the pH of the water in a neutral state.

Figs. 3 and 4 show the effect of contact time on the removal of calcium and magnesium ions by Purolite C-100 Na⁺ ion exchange resin. As shown in Figs. 3 and 4, the percentage of removal of calcium and magnesium ions increased over time. It also increased rapidly for different concentrations during the initial times, until the equilibrium is reached. Moreover, at contact time of 60 min, the removal percentage was 36.17%, 70.21%, 90.69% and 95.94% for calcium ions and 26.14%, 63.63%, 76.14%

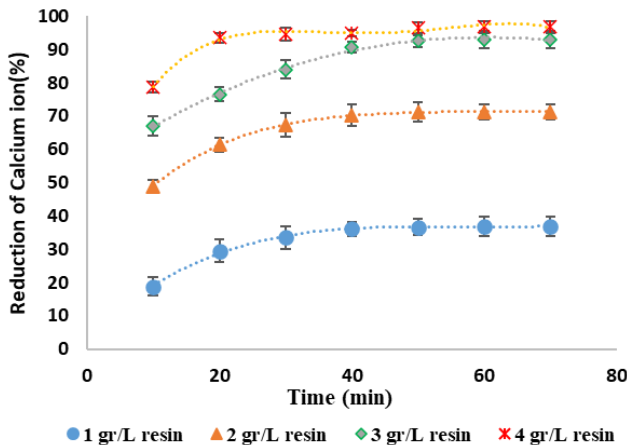


Fig. 3 The reduction of calcium ion versus contact time using Purolite C-100 Na^+ at 25°C and 350 rpm

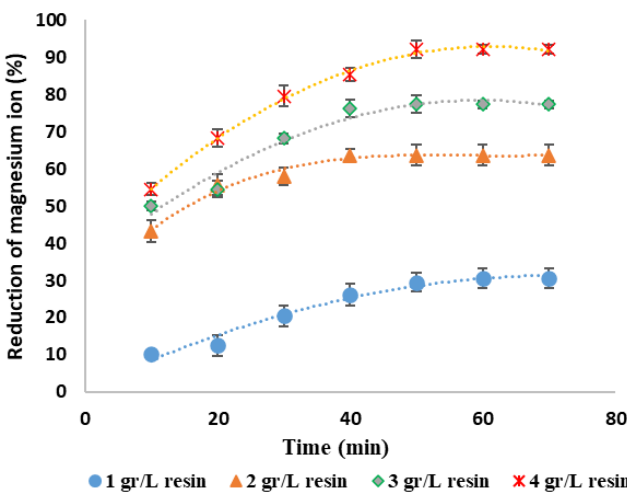


Fig. 4 The reduction of magnesium ion versus contact time using Purolite C-100 Na^+ at 25°C and 350 rpm

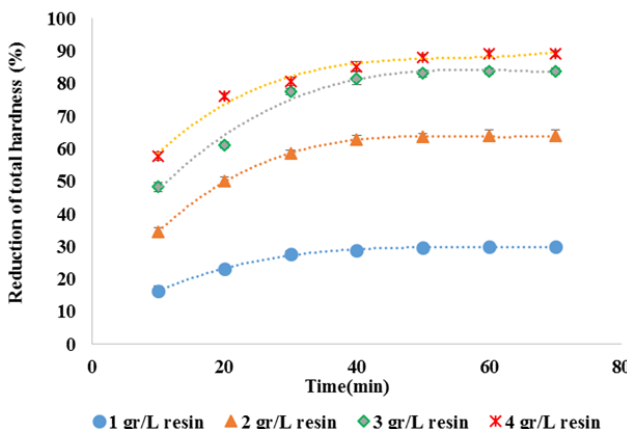


Fig. 5 The reduction of total hardness versus contact time using Ambersep IR252 H^+ at 25°C and 350 rpm

and 85.23% for magnesium ions, respectively. After that, increasing the contact time did not significantly affect the percentage of removal. The initial absorption rate is swift, due to a large number of active ion exchange resin sites for reacting with metal ions. This subject causes the absorption rate on the surface of the resin to increase, rapidly. As the

amount of remained ion on the surface decreases, the absorption rate is reduced due to the formation of repulsive forces between alkali metals on the solid surface and in the liquid phase, which is indicated by a horizontal line after 60 min. The metal removal charts are horizontal and continuous in time, suggesting a single layer coating of metal ions on the surface of the resin. The reactions carried out during the ion exchange process are as follows.

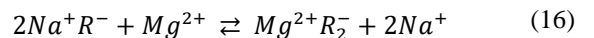
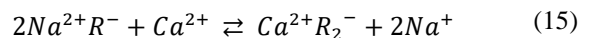


Fig. 5 illustrates the effect of contact time on the removal percentage of the total hardness by various concentrations of the Ambersep IR252 H^+ ion exchange resin. As shown in this fig, the reduction percentage of total hardness increased with increasing contact time. This trend continues until the process is equilibrated and then did not change, considerably. According to the figure, the removal percentage of total hardness with 1 g/L of resin was 29.96%, 2 g/L of resin was equivalent to 64.01%, 3 g/L of resin was equivalent to 83.84% and 4 g/L was equivalent to 89.22%. Therefore, it can be said that the optimal concentration in this experiment, like Purolite C-100 Na^+ resin, was 3 g/L of resin. Therefore, this resin was suitable for removal of water hardness, such as Purolite C-100 Na^+ resin, because it had high removal efficiency. The disadvantages of acid-based resins are that, by increasing the contact time, due to the release of hydrogen ion in water, the pH of the water becomes highly acidic. Therefore, at low pH, the amount of adsorption decreases. Because the surface of the resin has a higher positive charge, ion exchange occurs between protons and free calcium. On the other hand, ions with anionic groups react on the surface of the resin and reduce the number of desired compounds to remove calcium ions. This problem can be solved by using the anionic form and cationic resins in a combination or series to keeping the pH in a neutral state.

Figs. 6 and 7 depict the effect of contact time on the removal of calcium ions and magnesium ions by the Ambersep IR252 H^+ resin. As shown in Figs. 7 and 8, a decrease in the amount of calcium and magnesium ions in water increased over time. Also, the percentage of removal of absorbed metal ions during the initial times increased rapidly for different concentrations, until the equilibrium is reached. Also, for calcium and magnesium ions in 60 min, calcium ions (30.58%, 68.08%, 84.57% and 86.17%) and magnesium ion (21.59%, 40.9%, 69.32% and 82.82%) were removed. For both ions, the equilibrium set at 60 min. After that, the increase in contact time did not affect the removal percentage of ions.

Fig. 8 demonstrates the effect of contact time on the removal percentage of total hardness is shown by various concentrations of Amberlite IR120 H^+ cationic ion exchange resin. As shown in this fig, the reduction percentage of the total hardness increased with increasing contact time. This trend continues until the process equilibrate and then did not change significantly. Therefore, the optimal contact time was 60 min. According to Fig. 8,

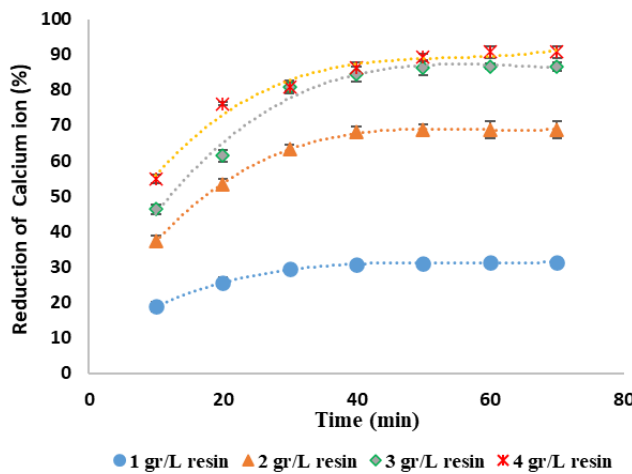


Fig. 6 The reduction of calcium ion versus contact time using Ambersep IR252 H⁺ at 25°C and 350 rpm.

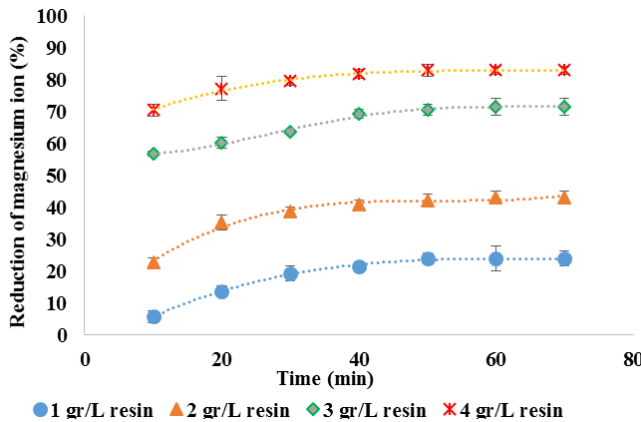


Fig. 7 The reduction of magnesium ion versus contact time using Ambersep IR252 H⁺ at 25°C and 350 rpm

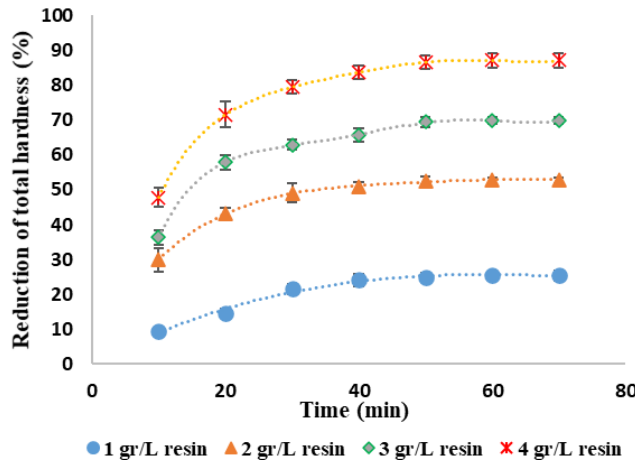


Fig. 8 The reduction of total hardness versus contact time using Amberlite IR120 H⁺ at 25°C and 350 rpm.

the removal percentage of total hardness with 1 g/L of resin was 25.43%, 2 g/L of resin was 52.5%, 3 g/L of resin was 69.63% and of 4 g/L was 87%. Therefore, according to the results, it can be said that the optimal concentration in this experiment, like the two resins used in the previous steps, was considered as 3 g/L.

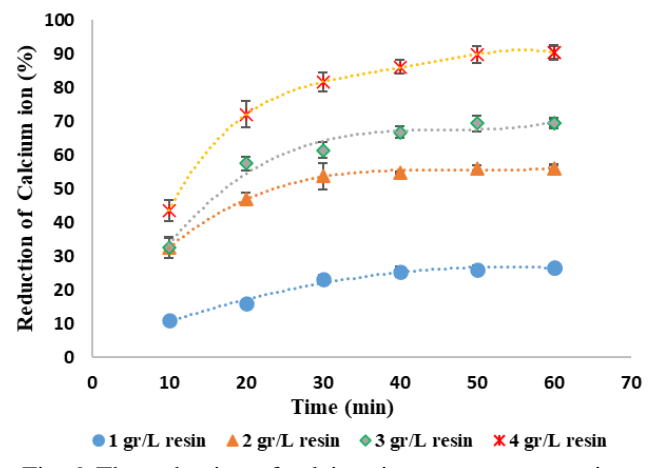


Fig. 9 The reduction of calcium ion versus contact time using Amberlite IR120 H⁺ at 25°C and 350 rpm

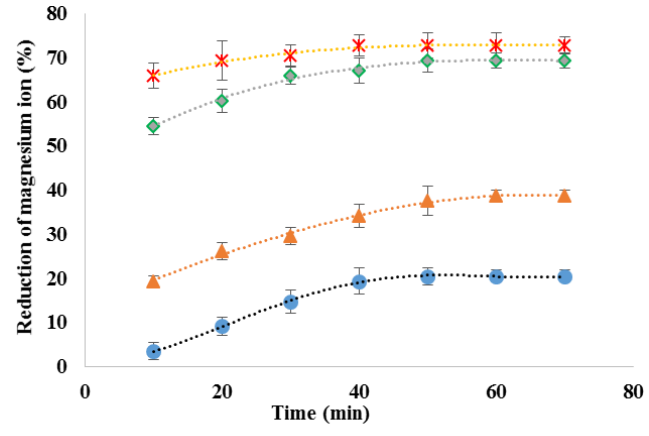


Fig. 10 The reduction of magnesium ion versus contact time using Amberlite IR120 H⁺ at 25°C and 350 rpm

Figs. 9 and 10 show the effect of contact time on the removal of calcium and magnesium ions by Amberlite IR120 H⁺ strong cationic resin. As shown in these figures, the percentage removal of calcium and magnesium ions in water increased over time. Also, the percentage of removal of the adsorbed metal ions increased rapidly over the initial times and then increased slowly until the equilibrium is reached. For calcium and magnesium ions at 60 min, by different concentrations of resin (1, 2, 3 and 4 g/L, the removal percentage were 25.27%, 54.79%, 66.76% and 86.17% for calcium ions and 19.32%, 34.09%, 67.04% and 72.72% for magnesium ion).

3.3 Comparison of the efficiency of cationic resins

The effectiveness of three ion exchange resins, Purolite C-100 Na⁺, Ambersep IR 252 H⁺, and Amberlite IR120 H⁺ were studied to reduce the total hardness. The results for optimum conditions (concentration of 3 g and contact time of 60 min) were illustrated in Fig. 11.

According to the results, the efficiency of the resins can be presented as follows:

Purolite C-100 Na⁺ > Ambersep IR 252 H⁺ > Amberlite IR 120 H⁺

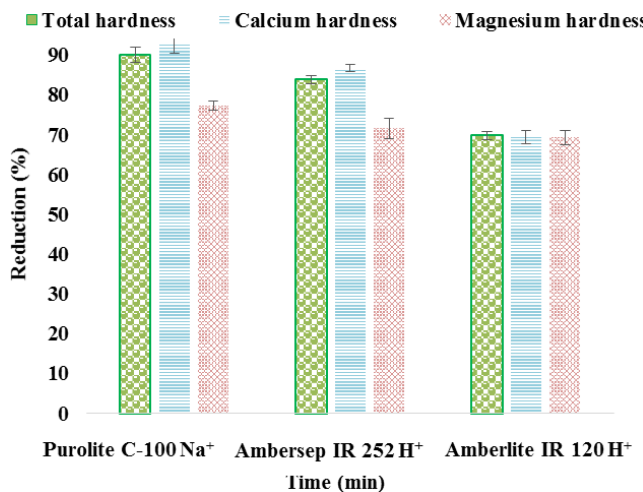


Fig. 11 The comparison of the removal percentage of total hardness, calcium ion and magnesium ion using strong cationic resins under optimum conditions

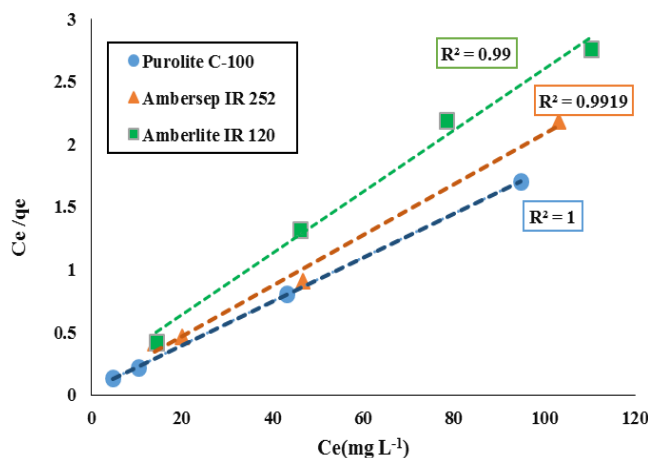


Fig. 12 The linear Langmuir isotherms for absorbing calcium ion using Purolite C-100 Na⁺, Ambersep IR 252 H⁺, and Amberlite IR 120 H⁺ under the experimental condition of constant initial concentration, 60 min contact time, 350 rpm, and 25°C

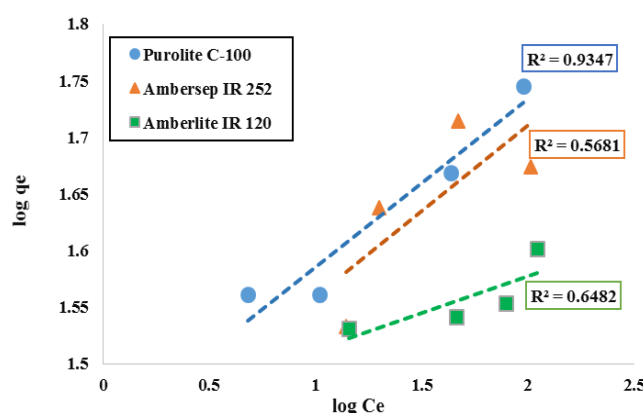


Fig. 13 The linear Freundlich isotherms for absorbing calcium ion using Purolite C-100 Na⁺, Ambersep IR 252 H⁺, and Amberlite IR 120 H⁺ under the experimental condition of constant initial concentration, 60 min contact time, 350 rpm and 25°C

As the results demonstrate, among the three strong cationic ion exchange resins, the Purolite C-100 Na⁺ resin had the highest removal percentage in reducing the total hardness and decreasing calcium and magnesium ions. It also keeps the water pH neutral. Therefore, this resin is selected as the best resin.

3.4 Study of the adsorption process equilibrium

Fig. 1 illustrates linear Langmuir isotherms for absorbing calcium ion using Purolite C-100 Na⁺, Ambersep IR 252 H⁺, and Amberlite IR 120 H⁺. In this figure, constant values of q_{\max} and K_L can be obtained by the slope and the intercept of the C_e/q_e in terms of C_e (Ebrahimi *et al.*, 2012, Gauthier *et al.*, 2012). All experiments occurred at the optimal contact time of 60 min, various concentrations (1, 2, 3, and 4 g/L) at 350 rpm, and 25 °C. It is obvious that, among the three strong cationic ion exchange resins were utilized in ion exchange experiments, only the Purolite C-100 Na⁺ ion exchange resin, with a high correlation coefficient of $R^2 = 1$, was better fitted with Langmuir linear curves than other resins. This subject shows that the Langmuir model was a suitable model for describing the mechanism of adsorption reaction of calcium ion by the Purolite C-100 Na⁺ resin. This item suggests that Langmuir's hypothesis is based on the homogeneous distribution of active sites on the surface of ion exchange resins. It is also possible to introduce the concept of ion exchange into the Langmuir model. The difference between the Langmuir model and the ion exchange method is that in the ion exchange process, all positions were initially occupied. The type of adsorption process can be described by the constant dimensionless R_L in Eq. (3), in which $R_L > 1$ shows an undesirable process, $R_L = 1$, the linear process, $0 < R_L < 1$ is a desirable process and $R_L = 0$, the process will be irreversible. Thus, in the process of adsorption of calcium ions by Purolite C-100 Na⁺ ion exchange resin, $R_L = 0.0172$ is obtained, which, by definition, indicates that the process of absorbing calcium ions from the aqueous solution by Purolite C-100 Na⁺ resin is possible and desirable. The Linear equation of Langmuir can be described as: (Dehghan *et al.* 2020).

$$\frac{C_e}{q_e} = \frac{1}{q_{\max}} \frac{1}{K_L C_i} \quad (17)$$

$$R_L = \frac{1}{1 + K_L C_i} \quad (18)$$

where, C_i (mg/L) and C_e (mg/L) are initial and equilibrium concentration at adsorption process, respectively. q_e (mg/g) is the amount of calcium adsorbed at equilibrium, q_{\max} (mg/g) is the maximum adsorption capacity, and K_L (L/mg) is Langmuir constant.

Fig. 13 presents Log (q_e) versus log (C_e). This Figure can be used to determine the values of n and K_F , which represent the slope and the intercept of the graph. The calculated values of the n and K_F constants, as well as the correlation coefficient R^2 , which represents the matching of

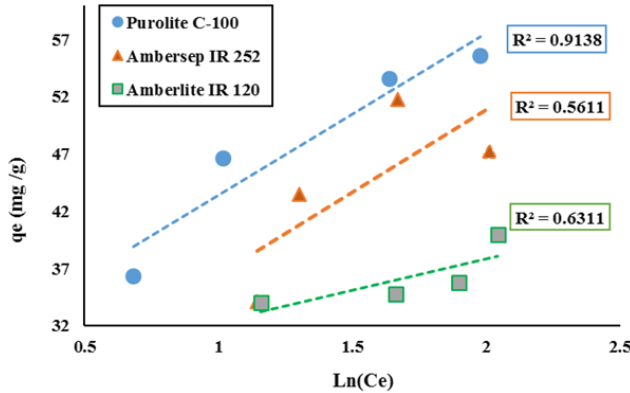


Fig. 14 The linear Temkin isotherms for absorbing calcium ion using Purolite C-100 Na^+ , Ambersep IR 252 H^+ and Amberlite IR 120 H^+ , under experimental condition of constant initial concentration, 60 min contact time, 350 rpm and 25°C

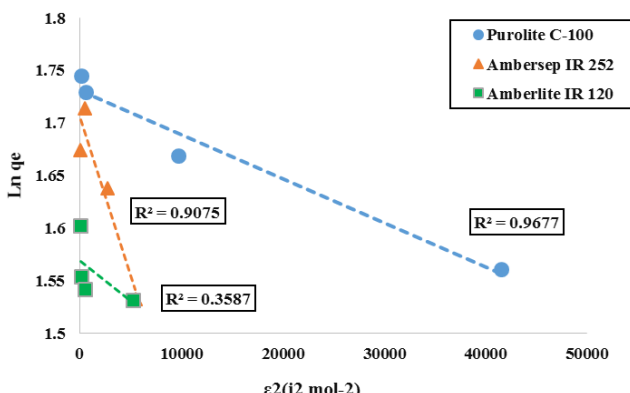


Fig. 15 The linear Dobinin-Radskvich isotherms for absorbing calcium ion using Purolite C-100 Na^+ , Ambersep IR 252 H^+ and Amberlite IR 120 H^+ under the experimental condition of constant initial concentration, 60 min contact time, 350 rpm, and 25°C

laboratory data with the isotherm model, which are given in Table 5.

As shown in Fig. 13, the equilibrium data for each of the three resins and the correlation coefficient were consistent with the Freundlich linear curve. As a result, the Purolite C-100 Na^+ ion exchange resin with a correlation coefficient of $R^2 = 0.9347$, was well suited to the Freundlich linear curve. This subject suggests that the Freundlich isotherm model can be a suitable model for describing the mechanism of calcium ion adsorption reaction by Purolite C-100 Na^+ ion exchange resin. Therefore, it can be said that the regions on the adsorbent surface are not uniform and that absorption sites have different absorption and absorption energy. Also, from the calculated constant n given in Table 4., which is between 2 and 10, it can be concluded that calcium ion adsorption by Purolite C-100 Na^+ ion exchange resin is a desirable process with suitable adsorption properties. The linear formula of Freundlich is presented as: (Dehghan *et al.* 2020, Omraei and Njafpour (2011)).

$$\log(q_e) = \log(K_F) + \frac{1}{n} \log(C_e) \quad (19)$$

where, K_F (L/mg) is the Freundlich model constant and n is the adsorption intensity.

In Fig. 14, the linear diagram of q_e is shown in terms of $\ln(C_e)$. The values of B and K_T can be obtained, which represent the slope and intercept, respectively (Zazouli, BarafrashtehPour, Sedaghat, & Mahdavi, 2013). Also, the calculated values of the B and K_T constants and the R^2 correlation coefficient, are reported in Table 4. As shown in Fig. 14, the experimental data for all three cationic ion exchange resins, with the given correlation coefficient, were in accordance with the Temkin model. As can be seen, from the three ion exchange resins used in the adsorption experiments, only the Purolite C-100 Na^+ ion exchange resin with a relatively high correlation coefficient, $R^2 = 0.9138$, was in good agreement with the Temkin equilibrium curve. Therefore, the Temkin isotherm model can be a suitable model for describing the mechanism of calcium ion adsorption reaction by Purolite C-100 Na^+ ion exchange resin. By comparison of the correlation coefficient between the Freundlich and Temkin models, it can be seen that Freundlich better describes the equilibrium of the calcium ion adsorption process with Purolite C-100 Na^+ ion exchange resin. Therefore, considering a logarithmic relation between enthalpy absorption and absorption coatings can be more logical than a linear relationship. The linear model of Temkin equation is represented as: (Dehghan *et al.* 2020 Omraei and Njafpour 2011).

$$q_e = BLnK_T + BLnC_e \quad (20)$$

$$B = \frac{RT}{b_T} \quad (21)$$

where, K_T (L/mg) is the Temkin constant and T (K) is temperature, R (8.314 J/mol K) is ideal gas constant, and b_T (J) is constant.

In Fig. 15, the $\ln(q_e)$ was depicted in terms of ϵ^2 , through which the constants β and q_{max} represent the slope and the intercept, can be calculated (Omraei and Njafpour 2011). The values of β and q_{max} constants, as well as the correlation coefficient R^2 , representing the compatibility of experimental data with the Dobinin-Radskvich model, Dubinin (1947) are reported in Table 4. The linear model of Dobinin-Radskvich is as below: (Dehghan *et al.* 2020, Omraei and Njafpour 2011).

$$\ln(q_e) = \ln(q_{max}) + \beta \ln(\epsilon^2) \quad (22)$$

$$\epsilon = RT \ln[1 + (\frac{1}{C_e})] \quad (23)$$

where, β (mol^2/J^2) is the activity coefficient related to mean adsorption energy and ϵ is the Polanyi potential.

As indicated in Fig. 15, the experimental data for all three ion exchange resins, with the obtained correlation coefficient, had coincidence with the Dobinin-Radskvich. It is also observed that among the three ion exchange resins in the adsorption experiments, only the Purolite C-100 Na^+ ion exchange resin with $R^2 = 0.9677$ was in good agreement with the Dobinin-Radskvich model compared to other

Table 4 The calculated constants for calcium ion adsorption using various resins according to isotherm models

Isotherm model	Calculated constants			Isotherm model	Calculated constants		
	R ²	q _{max} (mg.g ⁻¹)	K _L (mg.g ⁻¹)		R ²	n	K _F (mg.g ⁻¹)
Langmuir				Freundlich			
Purolite C-100 Na ⁺	1.0000	57.143	0.386	Purolite C-100 Na ⁺	0.9347	6.7520	27.378
Ambersep IR 252 H ⁺	0.9919	17.036	2.906	Ambersep IR 252 H ⁺	0.5681	14.475	25.609
Amberlite IR 120 H ⁺	0.99	7.0270	5.785	Amberlite IR 120 H ⁺	0.6482	5.4089	28.022
Temkin	R ²	B	K _T	Dobinin-Radskvich	R ²	B (mol ² j ⁻²)	q _{max} (mg.g ⁻¹)
Purolite C-100 Na ⁺	0.9138	14.139	7.940	Purolite C-100 Na ⁺	0.9677	4×10 ⁻⁶	5.65
Ambersep IR 252 H ⁺	0.5611	14.475	4.557	Ambersep IR 252 H ⁺	0.9075	3×10 ⁻⁵	5.51
Amberlite IR 120 H ⁺	0.6311	5.4730	136.2	Amberlite IR 120 H ⁺	0.3587	8×10 ⁻⁶	4.80

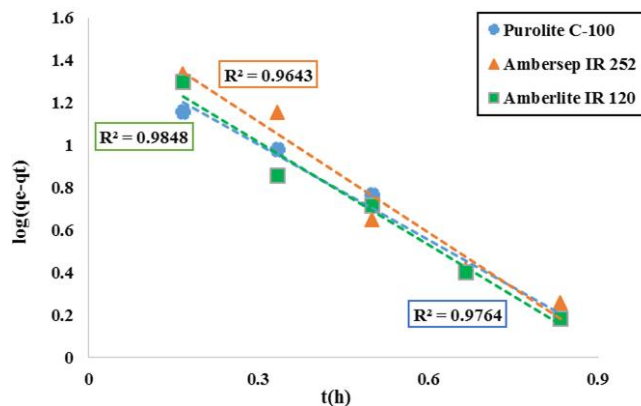


Fig. 16 The linear pseudo-first-order kinetic model for absorbing calcium ion using Purolite C-100 Na⁺, Ambersep IR 252 H⁺ and Amberlite IR 120 H⁺ under the experimental condition of constant initial concentration, 60 min contact time, 350 rpm, and 25°C

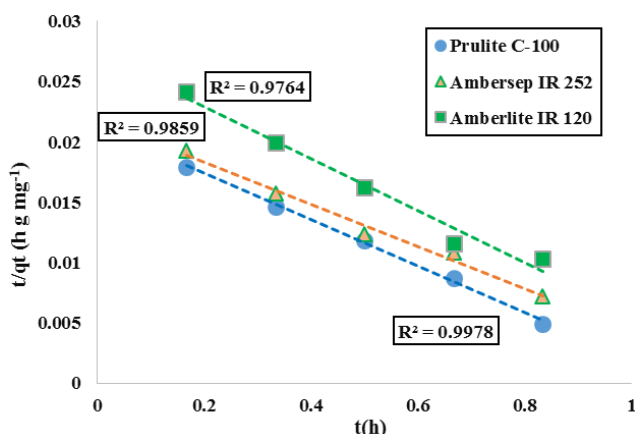


Fig. 17 The linear pseudo-second-order kinetic model for absorbing calcium ion using Purolite C-100 Na⁺, Ambersep IR 252 H⁺ and Amberlite IR 120 H⁺ under the experimental condition of constant initial concentration, 60 min contact time, 350 rpm, and 25°C

resins. This suggests that the Dobinin-Radskvich isotherm can be a suitable model for describing the mechanism of calcium ion adsorption reaction by Purolite C-100 Na⁺ resin.

The results of the study of adsorption isotherms including their constants and correlation coefficients are

reported in Table 4. As can be observed, by studying the equilibrium process of calcium ion adsorption, it can be found that the experimental data of ion exchangers of Purolite C-100 Na⁺ in comparison with other resins were relatively consistent with the linear curves of adsorption isotherms. Therefore, by comparing the models studied by the Purolite C-100 Na⁺, it can be seen that the Langmuir model describes the absorption process better than the Freundlich, Temkin and Dobinin-Radskvich models. Therefore, the Langmuir model with R²=1 was more suitable for prediction of adsorption behavior than other isotherm models. Comparison of maximum absorption capacity of the Langmuir model (57.143 mg/g) and the maximum theoretical absorption capacity of the Dobinin-Radskvich model (5.65 mg/g) with the maximum experimental absorption capacity (48.01 mg/g) indicates that the Langmuir model describes the absorption mechanism better than other models.

3.5 Study of the kinetics of the adsorption process

As shown in Fig. 16, the obtained experimental data for all three ion exchange resins at the optimum concentration of 3 g/L, 350 rpm and 25°C, are matched with low R² on the graphs, which shows that the Pseudo-first-order model, was not a suitable model for describing the kinetics of the adsorption reaction of calcium ions by resins. Therefore, it can be concluded that the intensity of filling adsorbent sites is not proportional to the empty sites. Moreover, taking into account the linear driving force for the process of adsorption of calcium ions by different ion exchange resins used in this paper is not logical.

According to Fig. 17, the obtained experimental data for each of the three ion exchange resins well matched to the model with a good correlation coefficient. This subject suggests that the pseudo-second-order model was a suitable model for describing the kinetics of the adsorption reaction of calcium ion by ion exchange resins. Therefore, it can be said that the intensity of filling of adsorbent sites is proportional to the square of the number of vacant free adsorbent sites, and the chemical reaction stage is also a process of controlling the absorption of calcium ions by resins.

In Fig. 18, the obtained data for each of the three ion exchange resins employed during the adsorption process

Table 5 The calculated constants for calcium ion adsorption using various resins according to adsorption kinetic models

Kinetic model		Calculated constants	
Pseudo-first-order	R ²	q _e (mg.g ⁻¹)	K _I (h ⁻¹)
Purolite C-100 Na ⁺	0.9848	28.151	3.437
Ambersep IR 252 H ⁺	0.9643	42.983	4.013
Amberlite IR 120 H ⁺	0.9764	31.311	3.701
Pseudo-second-order	R ²	q _e (mg.g ⁻¹)	K ₂ (gmg ⁻¹ h ⁻¹)
Purolite C-100 Na ⁺	0.9978	52.083	0.1843
Ambersep IR 252 H ⁺	0.9859	57.143	0.0712
Amberlite IR 120 H ⁺	0.9764	46.296	0.0833
Morris-Webber	R ²	C (mg.g ⁻¹)	k _{id} (m ^{gg} ⁻¹ h ^{-0.5})
Purolite C-100 Na ⁺	0.9865	23.117	26.42
Ambersep IR 252 H ⁺	0.9303	7.0487	42.34
Amberlite IR 120 H ⁺	0.8718	4.8252	35.03

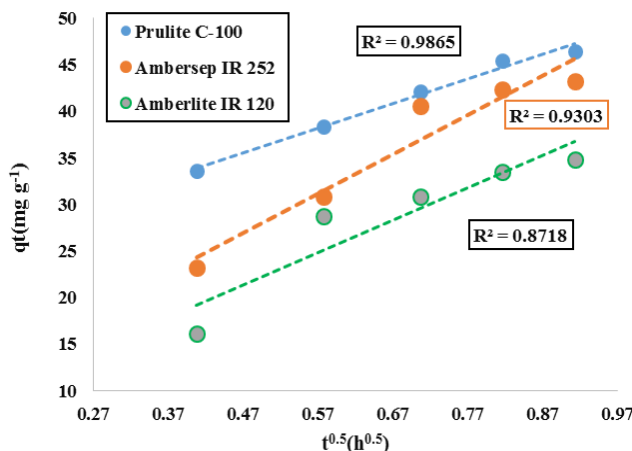


Fig. 18 The morris-Webber kinetic model for absorbing calcium ion using Purolite C-100 Na⁺, Ambersep IR 252 H⁺ and Amberlite IR 120 H⁺ under the experimental condition of constant initial concentration, 60 min contact time, 350 rpm, and 25°C

have coincided with a relatively favorable correlation coefficient on the graphs. Regarding the linearity of the diagrams, it can be said that the intrinsic penetration of one of the control steps is the rate of reaction of the calcium ion adsorption reaction with ion exchange resins, but because the graph has not crossed the intercept, the intrinsic penetration is not the only factor controlling the reaction velocity.

Table 5 shows the calculated kinetic constants for three strong cationic ion exchange resins. The results show that the experimental data for the Purolite C-100 Na⁺ ion exchange resin with a relatively high R² was adapted to linear curves of absorption kinetics models. Also, this type of resin had a good fit with the pseudo-second-order model. This suggests that the hypothesis of the pseudo-second-order kinetic model dominates the reaction of calcium absorption on ion exchange resins. The velocity limiting step in this process was the chemical absorption reaction, which involves exchanging electrons. In this regard, it can

be said that in adsorption processes from aqueous solution by an adsorbent, when the concentration of the absorbing material in aqueous solution was high, the dominant model was pseudo-first-order model. However, in low concentrations, the adsorption process had consistency with the pseudo-second-order model. Experimental data also had a good fit for the Purolite C-100 Na⁺ resin with the Morris-Weber kinetic model (Weber *et al.* 1963), which also indicates that another limiting step in the reaction was the intrusive penetration. Thus, it can be said that the process of adsorption of calcium on ion exchange resins occurs during two phases of physical absorption and chemical absorption.

3.6 Performance of cationic IR 252 H⁺ resins and anionic 402 OH⁻ resin in the combination process

In this section, cationic and anionic ion exchange type resins (H⁺ and OH⁻) were utilized in the combination stage. Cationic resins have replaced calcium and magnesium ions with mobile cationic ions. Anionic resins also have conducted ion exchange with anions in water, often chlorine ions, bicarbonate, and sulfate. In the previous experiments, cationic resins evaluated, separately. Although the cationic H⁺ resin had a good performance in reducing the hardness, it released H⁺ ion in water causes pH to become strongly acidic. At this stage, for neutralization and reduction of electrical conductivity, the experiments were carried out at a concentration of 3 g/L of cationic resin. Then with different concentrations (3, 6, 9, and 12 grams per liter) of anionic resins all the experiments were investigated at contact time (10, 20, 30, 40, 50, 60 and 70 min), the results of which have been reported in Table 6.

Table 6 presents the results of cationic and anionic resins for various parameters (pH, EC, TDS). At a concentration of 3 g/L of cationic resin and 3 g/L of anionic resin, the solution pH decreased with increasing time due to the competition between calcium ions and magnesium ions released in water with H⁺ ion. Therefore, this amount of released H⁺ ion during the ion exchange process shows that adsorption may also occur on the surface of the resin, in

Table 6 The results of the performance of cationic IR 252 H⁺ and anionic IRA 402 OH⁻ resins in combination stage

Adsorbent (g)		Contact time (minute)						
		10	20	30	40	50	60	70
3 g/L cationic resin+ 3 g/L anionic resin	pH	3.12	2.83	2.75	2.69	2.65	2.63	2.62
	TDS(ppm)	575	545	519	489	455	424	418
	EC($\mu\text{s}/\text{cm}$)	884.0	959.0	1021	1137	1178	1195	1223
3 g/L cationic resin+ 6 g/L anionic resin	pH	4.50	4.65	4.93	5.15	5.25	5.27	5.35
	TDS(ppm)	485.3	442.0	428.0	378.0	342.0	320.0	305.0
	EC($\mu\text{s}/\text{cm}$)	596	535	514	485	435	425	412
3 g/L cationic resin+ 9 g/L anionic resin	pH	5.50	5.75	5.93	6.15	6.25	6.32	6.39
	TDS(ppm)	472.5	330.0	311.0	302.0	245.0	235.15	217.15
	EC($\mu\text{s}/\text{cm}$)	576	425	398	385	318	309	305
3 g/L cationic resin+ 12 g/L anionic resin	pH	6.25	6.33	6.57	6.95	7.35	7.53	7.61
	TDS(ppm)	385	315	255	218	198	175	168
	EC($\mu\text{s}/\text{cm}$)	519	403	309	286	259	225	215

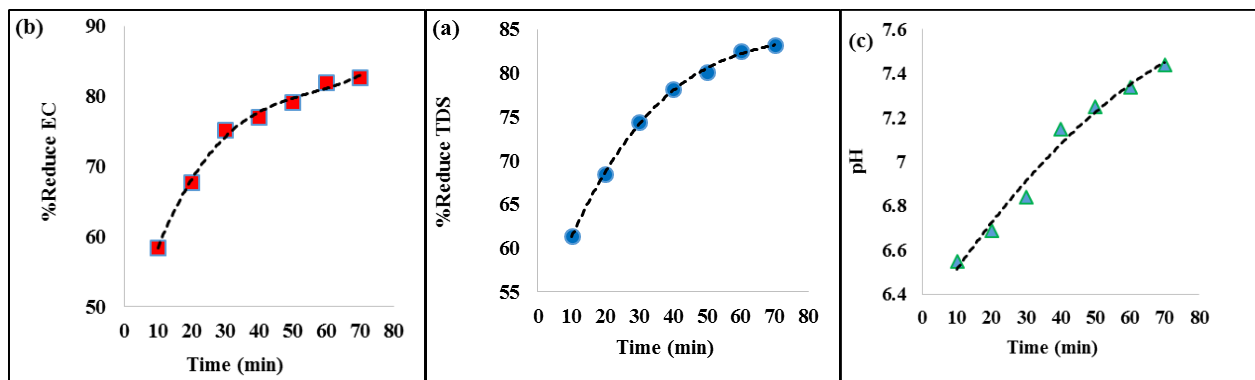


Fig. 19 The reduction of (a) TDS, (b) EC and (c) pH at optimum concentration, (3 g/L cationic resin and 12 g/L anionic resin)

addition to ion exchange. Therefore, it is necessary to use higher concentrations of anion to bring the pH of the water to a neutral state. The results showed higher concentrations of anionic resins, so that, by releasing more OH⁻ ions, more bonds are created with H⁺ ion. This phenomenon causes the pH to be neutralized earlier, so the 3 g/L cationic resin and 12 g/L anionic resin was considered to be the best concentration for better pH adjustment.

The results of ion exchange resins in combination process in best concentration (3 g/L cationic resin and 12 g/L anionic resin) for pH, EC, TDS parameters, is shown in Fig. 19. Considering the different concentrations studied for ion exchange resins, (3 g/L cationic resin and 12 g/L anionic resin) were considered as the best concentration. Because the pH of the water has been neutralized, as well as the electrical conductivity and TDS decreased with increasing time.

In this part, the performance of resins was evaluated as series mode experiments. The experimental conditions for these tests are similar to the combined phase, with a difference that at this stage, the water sample was first tested from the cationic resin bed and passed through the

specified residence time of the anionic resin bed. This stage, like the previous stage, was optimized at a concentration of 3 g/L, from which the cationic resins were investigated separately from the first stage, then with different concentrations (3, 6, 9, and 12 g/L) the performance of the anionic resin was investigated at the contact time (10, 20, 30, 40, 50, 60, and 70 min), and the results are reported in Table 7.

In Table 7 the results of cationic resins H⁺ and anionic OH⁻ are given in series for different parameters (pH, EC, TDS). The results, like the combined method, show that at a concentration of 3 g/L of cationic resin and 3 g/L of anionic resin, the solution pH decreased with increasing time, because of the competition between ions released from calcium and magnesium in water. Therefore, this amount of ion is released during the ion exchange process shows that adsorption may also occur on the surface of the resin, in addition to the ion exchange. Therefore, it is necessary to use higher concentrations of anion to bring the pH of the water to neutral state. The results show that the higher concentrations of anionic resins gives better result, and by releasing more OH⁻ ion, it makes stronger bonds with H⁺

Table 7 The results of the performance of cationic IR 252 H⁺ and anionic IRA 402 OH⁻ resins in series model

Adsorbent (g)		Contact time (minute)						
		10	20	30	40	50	60	70
3 g/L cationic resin+ 3 g/L anionic resin	pH	4.35	4.15	3.93	3.74	3.52	3.42	3.27
	TDS(ppm)	584	556	524	504	462	432	424
	EC($\mu\text{s}/\text{cm}$)	895	962	1032	1148	1198	1212	1232
3 g/L cationic resin+ 6 g/L anionic resin	pH	5.55	5.79	6.96	6.18	6.28	6.35	6.56
	TDS(ppm)	495	462	435	388	352	342	318
	EC($\mu\text{s}/\text{cm}$)	608	545	508	495	465	432	419
3 g/L cationic resin+ 9 g/L anionic resin	pH	6.55	6.69	6.84	7.15	7.25	7.34	7.44
	TDS(ppm)	485	350	325	311	265	243	227
	EC($\mu\text{s}/\text{cm}$)	596	528	432	397	345	332	315
3 g/L cationic resin+ 12 g/L anionic resin	pH	6.95	7.11	7.18	7.32	7.48	7.58	7.64
	TDS(ppm)	395	338	282	225	195	183	173
	EC($\mu\text{s}/\text{cm}$)	535	515	465	432	365	324	305

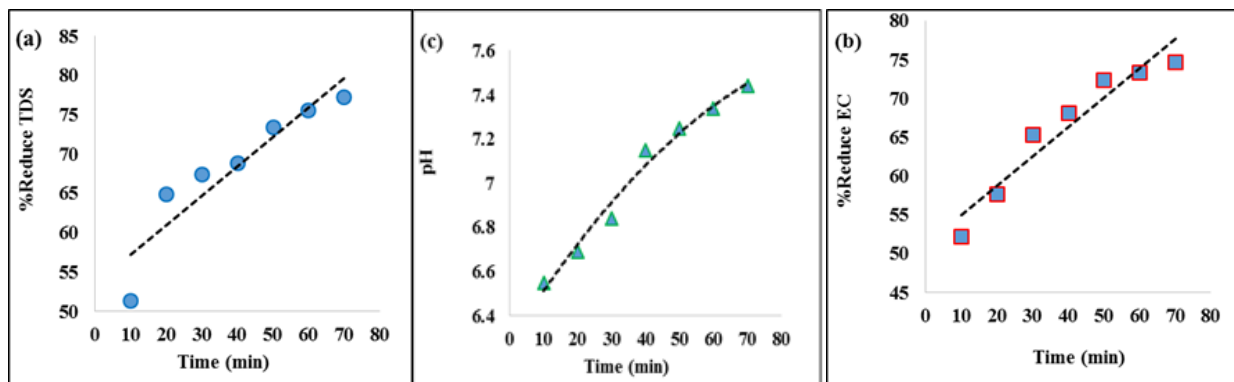


Fig. 20 The reduction of (a) TDS, (b) EC and (c) pH at optimum concentration, (3 g/L cationic resin and 12 g/L anionic resin)

ion. Therefore, from the studied concentrations, (3 g/L of cationic resin, 12 g/L of anionic resin) were selected as the best concentration, which was better in adjusting the pH of the water.

The results of the ion exchange resins were summarized in the optimum concentration (3 g/L cationic resin, 9 g/L anionic resin) for pH, EC, and TDS parameters in Fig. 20. Considering the different studied concentrations for ion exchange resins, (3 g/L of cationic H⁺ resin and 9 g/L of anionic OH⁻ resin) were considered as the best concentrations.

4. Conclusion

In this research, performance efficiency, modeling of the adsorption process equilibrium and study of the kinetics of the adsorption process for Purolite C-100 H⁺, Ambersep IR 252 H⁺, and Amberlite IR 120 H⁺ cationic resins for reduction of hardness in drinking water of Bushehr city, Iran, were investigated. The adsorption efficiency was obtained at optimal time of 60 min at different

concentrations of resins equal to 1, 2, 3, and 4 g/L results showed that by using Purolite C-100 Na⁺ resin, the best reduction percentage in total hardness was 93.085%; and the best percentages of calcium and magnesium ions reduction were 95.91% and 92.545%, respectively. For Ambersep IR 252 H⁺ resin: the best reduction of total hardness was 89.22% and the best percentages of calcium and magnesium ions reduction were 90.69% and 82.95% respectively. Also, for the Amberlite IR120 H⁺ resin, reduction percentage of the total hardness at the best condition 87.07% and the reduction in calcium and magnesium ions was 90.43% and 72.73% respectively. According to the results, the Purolite C-100 Na⁺ resin had the best performance in reducing the hardness of calcium and magnesium ions. Experimental data have the best fit with Pseudo-second-order kinetic models. Also, due to the good matching of the data with the Morris-Weber model and the linearity of the diagram, it can be said that the intrinsic penetration stage is one of the steps in controlling the velocity of this reaction. Thus both chemical absorption and physical absorption are involved in trapping calcium ions. It was found that the Langmuir had good agreement

with experimental data. The results showed that the Purolite C-100 Na⁺ resins, although had a good performance in reducing the hardness, caused a decrease in water pH and an increase in EC due to the release of hydrogen ion. Therefore, ion exchange resins have been used in combination and series to regulate and reduce EC. The results also showed that in the combination method (3 g/L cation and 12 g/L anion) can reduce the TDS of water from 686 to almost 170 ppm.

References

- Ambashta, R.D. and Sillanpää, M. (2010), "Water purification using magnetic assistance: a review", *J. Hazard. Mater.*, **180**(1-3), 38-49.
<https://doi.org/10.1016/j.hazmat.2010.04.105>.
- Apell, J.N. and Boyer, T.H. (2010), "Combined ion exchange treatment for removal of dissolved organic matter and hardness", *Water Res.*, **44**(8), 2419-2430.
<https://doi.org/10.1016/j.watres.2010.01.004>.
- Asl, S. H., Ahmadi, M., Ghiasvand, M., Tardast, A. and Katal, R. (2013), "Artificial neural network (ANN) approach for modeling of Cr (VI) adsorption from aqueous solution by zeolite prepared from raw fly ash (ZFA)", *J. Ind. Eng. Chem.*, **19**(3), 1044-1055.
<https://doi.org/10.1016/j.jiec.2012.12.001>.
- American Public Health Association, American Water Works Association, Water Pollution Control Federation and Water Environment Federation (1912), *Standard Methods for the Examination of Water and Wastewater*, American Public Health Association, Washington, D.C., U.S.A.
- Benefield, L.D., Judkins, J.F. and Weand, B.L. (1982), *Process Chemistry for Water and Wastewater Treatment*, Prentice-Hall, New Jersey, U.S.A.
- Coca, M., Mato, S., González-Benito, G., Urueña, M.Á. and García-Cubero, M.T. (2010), "Use of weak cation exchange resin Lewatit S 8528 as alternative to strong ion exchange resins for calcium salt removal", *J. Food Eng.*, **97**(4), 569-573.
<https://doi.org/10.1016/j.jfoodeng.2009.12.002>.
- Comstock, S.E. and Boyer, T.H. (2014), "Combined magnetic ion exchange and cation exchange for removal of DOC and hardness", *Chem. Eng. J.*, **241**, 366-375.
<https://doi.org/10.1016/j.cej.2013.10.073>.
- Cornelissen, E., Beerendonk, E., Nederlof, M., Van der Hoek, J. and Wessels, L. (2009), "Fluidized ion exchange (FIX) to control NOM fouling in ultrafiltration", *Desalination*, **236**(1-3), 334-341. <https://doi.org/10.1016/j.desal.2007.10.084>.
- Dehghan, P., Abbasi, M., Mofarahi, M. and Azari, A. (2020), "Adsorption of synthetic and real Kinetic Hydrate Inhibitors (KHI) wastewaters on activated carbon: Adsorption kinetics, isotherms, and optimized conditions", *Sep. Sci. Technol.*, **56**(13), 2266-2277.
<https://doi.org/10.1080/01496395.2020.1821220>.
- Dubinin, M. (1947), "The equation of the characteristic curve of activated charcoal", *Dokl. Akad. Nauk. SSSR.*, **55**, 327-329.
- Duncan, J. and Lister, B. (1948), "Ion exchange", *Quarterly Rev. Chem. Soc.*, **2**(4), 307-348.
<https://doi.org/10.1039/QR9480200307>.
- Ebrahimi, A., Kamarehie, B., sgari, G., Seid, M.A. and Roshanawi, G. (2012), "Drinking water corrosivity and sediment in the distribution network of Kuhdasht, Iran", *Health Syst. Res.*, **8**(3), 480-486.
- Entezari, M.H. and Tahmasbi, M. (2009), "Water softening by combination of ultrasound and ion exchange", *Ultrason. Sonochem.*, **16**(3), 356-360.
- <https://doi.org/10.1016/j.ulsonch.2008.09.008>.
- Gauthier, G., Chao, Y., Horner, O., Alos-Ramos, O., Hui, F., Lédition, J. and Perrot, H. (2012), "Application of the fast controlled precipitation method to assess the scale-forming ability of raw river waters", *Desalination*, **299**, 89-95.
<https://doi.org/10.1016/j.desal.2012.05.027>
- Gupta, S.S. and Bhattacharyya, K.G. (2008), "Immobilization of Pb (II), Cd (II) and Ni (II) ions on kaolinite and montmorillonite surfaces from aqueous medium", *J. Environ. Manage.*, **87**(1), 46-58. <https://doi.org/10.1016/j.jenvman.2007.01.048>.
- Hadi, M. (2010), "Development a software for calculation of eight important water corrosion indices", *Proceedings of the 12th National Conference on Environmental Health*, Tehran, Iran, November.
- Hayani, A., Mountadar, S., Tahiri, S. and Mountadar, M. (2016), "Softening of hard water by ion-exchange with strongly acidic cationic resin. Application to the brackish groundwater of the coastal area of El Jadida province (Morocco)", *J. Mater. Environ. Sci.*, **7**(10), 3875-3884.
- Helms, R.F. (1973), "Evaluation of ion exchange for demineralization of wastewater", M.Sc. Dissertations, University of Colorado, Colorado, U.S.A.
- Ismail, N.N. (2016), "Experimental study on ion exchange rate of calcium hardness in water softening process using strong acid resin DOWEX HCR S/S", *Al-Nahrain J. Eng. Sci.*, **19**(1), 107-114.
- Katal, R. and Pahlavanzadeh, H. (2011), "Zn (II) ion removal from aqueous solution by using a polyaniline composite", *J. Vinyl Addit. Technol.*, **17**(2), 138-145.
<https://doi.org/10.1002/vnl.20252>.
- Khan, M.I., Wu, L., Mondal, A.N., Yao, Z., Ge, L. and Xu, T. (2016), "Adsorption of methyl orange from aqueous solution on anion exchange membranes: Adsorption kinetics and equilibrium", *Membr. Water Treat.*, **7**(1), 23-38.
<http://doi.org/10.12989/mwt.2016.7.1.023>.
- Khan, M.I., Ansari, T.M., Zafar, S., Buzdar, A.R., Khan, M.A., Mumtaz, F., Prapamonthon, T. and Akhtar, M. (2018), "Acid green-25 removal from wastewater by anion exchange membrane: Adsorption kinetic and thermodynamic studies", *Membr. Water Treat.*, **9**(2), 79-85.
<https://doi.org/10.12989/mwt.2018.9.2.079>.
- Lv, R., Hu, Y., Li, R., Zhang, X., Liu, J., Fan, C., Feng, J., Jhang, L. and Wang, Z. (2019), "Adsorption of Ca²⁺ and Mg²⁺ ions from phosphoric acid-nitric acid solution using strong acid cation resin in fixed bed column", *Desalin. Water Treat.*, **155**, 225-236. <http://doi.org/10.5004/dwt.2019.23919>.
- Millar, G.J., Papworth, S. and Couperthwaite, S.J. (2014), "Exploration of the fundamental equilibrium behaviour of calcium exchange with weak acid cation resins", *Desalination*, **351**, 27-36. <https://doi.org/10.1016/j.desal.2014.07.022>.
- Millar, G.J., Couperthwaite, S.J., De Bruyn, M. and Leung, C.W. (2015), "Ion exchange treatment of saline solutions using Lanxess S108H strong acid cation resin", *Chem. Eng. J.*, **280**, 525-535. <https://doi.org/10.1016/j.cej.2015.06.008>.
- Omraei, M. and Najafpour, G.D. (2011), "Removal of zinc from aqueous phase by charcoal ash", *World Appl. Sci. J.*, **13**(2), 331-340.
- Özmetin, C. and Aydin, O. (2007), "A semi-empirical model for adsorption of magnesium ion from magnesium impurity-containing saturated boric acid solutions on amberlite IR-120 resin" *Fresenius Environ. Bull.*, **16**(7), 720-725.
- Özmetin, C., Aydin, Ö., Kocakerim, M.M., Korkmaz, M. and Özmetin, E. (2009), "An empirical kinetic model for calcium removal from calcium impurity-containing saturated boric acid solution by ion exchange technology using Amberlite IR-120 resin", *Chem. Eng. J.*, **148**(2-3), 420-424.
<https://doi.org/10.1016/j.cej.2008.09.021>.

- Prajapati, M., Gaur, P. and Dasare, B. (1983), "Water-softening by continuous counter-current ion-exchange single column technique", *Desalination*, **48**(3), 281-292.
[https://doi.org/10.1016/0011-9164\(83\)85004-8](https://doi.org/10.1016/0011-9164(83)85004-8).
- Sepehr, M.N., Zarrabi, M., Kazemian, H., Amrane, A., Yaghmaian, K. and Ghaffari, H.R. (2013), "Removal of hardness agents, calcium and magnesium, by natural and alkaline modified pumice stones in single and binary systems", *Appl. Surf. Sci.*, **274**, 295-305.
<https://doi.org/10.1016/j.apsusc.2013.03.042>.
- Shams, M., Mohamadi, A. and Sajadi, S.A. (2012), "Evaluation of corrosion and scaling potential of water in rural water supply distribution networks of Tabas, Iran", *World Appl. Sci. J.*, **17**(11), 1484-1489.
- Townsend, R.P. (1993), *Fundamentals of Ion Exchange in Ion Exchange Processes: Advances and applications*, U.K.
- Vairavamoorthy, K., Yan, J., Galgale, H. M. and Gorantiwar, S. D. (2007), "IRA-WDS: A GIS-based risk analysis tool for water distribution systems", *Environ. Model. Softw.*, **22**(7), 951-965.
<https://doi.org/10.1016/j.envsoft.2006.05.027>.
- Weber, W.J. and Morris, J.C. (1963), "Kinetics of adsorption on carbon from solution", *J. Sanitary Eng. Division*, **89**(2), 31-60.
- Yu, Z., Qi, T., Qu, J. and Guo, Y. (2015), "Application of mathematical models for ion-exchange removal of calcium ions from potassium chromate solutions by Amberlite IRC 748 resin in a continuous fixed bed column", *Hydrometallurgy*, **158**, 165-171. <https://doi.org/10.1016/j.hydromet.2015.10.015>.
- Zainol, Z. and Nicol, M.J. (2009), "Ion-exchange equilibria of Ni^{2+} , Co^{2+} , Mn^{2+} and Mg^{2+} with iminodiacetic acid chelating resin Amberlite IRC 748", *Hydrometallurgy*, **99**(3-4), 175-180.
<https://doi.org/10.1016/j.hydromet.2009.08.004>
- Zazouli, M., BarafrashtehPour, M., Sedaghat, F. and Mahdavi, Y. (2013), "Assessment of scale formation and corrosion of drinking water supplies in Yasuj (Iran) in 2012", *J. Mazandaran Univ. Med. Sci.*, **22**(2), 100-108.
- Zuo, K., Yuan, L., Wei, J., Liang, P. and Huang, X. (2013), "Competitive migration behaviors of multiple ions and their impacts on ion-exchange resin packed microbial desalination cell", *Bioresource Technol.*, **146**, 637-642.
<https://doi.org/10.1016/j.biortech.2013.07.139>.